Extended Abstracts of the 2018 International Conference on Solid State Devices and Materials, Tokyo, 2018, pp1069-1070

Crystallographic, optical, and electronic properties of $Cu(In,Ga)Se_2$ and Cu-deficient phases, $Cu(In,Ga)_3Se_5$ and $Cu(In,Ga)_5Se_8$ in Cu_2Se-$(In,Ga)_2Se_3$ pseudo-binary System

Tsuyoshi Maeda, Kenta Ueda, and Takahiro Wada

Department of Materials Chemistry, Ryukoku University
Seta, Otsu, 520-2194, Japan
Phone: +81-77-543-7468 E-mail: tmaeda@ad.ryukoku.ac.jp

Abstract

We obtained single-phase $Cu(In_{1-x}Ga_x)Se_2$ ($0.0 \leq x \leq 1.0$) solid solution samples with chalcopyrite-type structure, and $Cu(In_{1-x}Ga_x)_3Se_5$ ($0.0 \leq x \leq 0.8$) and $Cu(In_{1-x}Ga_x)_5Se_8$ ($0.5 \leq x \leq 1.0$) samples with stannite-type structure. Their energy levels of the valence band maximum (VBM) were measured by photoemission yield spectroscopy (PYS). The VBM levels of the $Cu(In_{1-x}Ga_x)Se_2$, $Cu(In_{1-x}Ga_x)_3Se_5$ and $Cu(In_{1-x}Ga_x)_5Se_8$ solid solution systems did not change significantly with Ga content, x. The energy levels of the VBM of the $Cu(In,Ga)_3Se_5$ and $Cu(In,Ga)_5Se_8$ systems were deeper than that of $Cu(In,Ga)Se_2$ system. The energy levels of the conduction band minimum (CBM) of the $Cu(In_{1-x}Ga_x)Se_2$, $Cu(In_{1-x}Ga_x)_3Se_5$ and $Cu(In_{1-x}Ga_x)_5Se_8$ systems increased with the Ga content.

1. Introduction

Recently, we reported the crystallographic and optical properties of $CuInSe_2$, $CuIn_3Se_5$, and $CuIn_5Se_8$ phases in the Cu_2Se-In_2Se_3 system [1, 2]. The band-gap energies of Cu-poor Cu-In-Se samples, i.e., $CuIn_3Se_5$ (1.17 eV) and $CuIn_5Se_8$ (1.22-1.24 eV), were wider than that of chalcopyrite-type $CuInSe_2$ (0.99 eV). The valence band maximum (VBM) level of the Cu-poor Cu-In-Se samples significantly decreased with decreasing Cu/In ratio. In order to fabricate high efficiency CIGSe solar cells, we should control the band alignment of $CdS/Cu(In,Ga)_3Se_5/Cu(In,Ga)Se_2$ interface in the CIGSe solar cells [3]. However, the existence regions, optical properties and electronic structures of $Cu(In,Ga)Se_2$, $Cu(In,Ga)_3Se_5$ and $Cu(In,Ga)_5Se_8$ solid solution systems are still under discussion. The objective of this research is to clarify the crystallographic and optical properties, and band diagrams of Cu-deficient compounds, $Cu(In,Ga)_3Se_5$ and $Cu(In,Ga)_5Se_8$ and to compare the obtained results with those of $Cu(In,Ga)Se_2$.

2. Experimental Procedures

We synthesized $Cu(In,Ga)Se_2$ and Cu-deficient $Cu(In,Ga)_3Se_5$ and $Cu(In,Ga)_5Se_8$ samples (x=0.0, 0.1, 0.2, 0.3, 0.4, 0.5, 0.6, 0.7, 0.8, 0.9, 1.0). $Cu(In_{1-x}Ga_x)Se_2$, $Cu(In_{1-x}Ga_x)_3Se_5$ and $Cu(In_{1-x}Ga_x)_5Se_8$ powder samples with $0.0 \leq x \leq 1.0$ were prepared by mixing the elemental Cu, In, Ga, and Se powders and sequential heating at 550 ºC. The phases in the powders were identified by X-ray powder diffraction (XRD). The band-gap energies of the Cu-poor samples were determined from the diffuse reflectance spectra of the ultraviolet-visible-near infrared spectroscopy. To understand the band diagram of the ZnO/CdS/CIGSe system, the ionization energies were measured by photoemission yield spectroscopy (PYS). Then, we determined the energy positions of the VBM and CBM of the $Cu(In,Ga)Se_2$, $Cu(In,Ga)_3Se_5$ and $Cu(In,Ga)_5Se_8$ samples from the vacuum level. Then, we discuss band alignment of $ZnO/CdS/Cu(In,Ga)Se_2$ solar cells with and without insertion of Cu-poor $Cu(In,Ga)_3Se_5$ layer.

3. Results and discussion

3.1 Crystal phases of $(1-y)Cu_2Se$-$y(In_{1-x}Ga_x)_2Se_3$ samples in the Cu_2Se-In_2Se_3-Ga_2Se_3 pseudo-ternary system

The phases in the $(1-y)Cu_2Se$-$y(In_{1-x}Ga_x)_2Se_3$ samples in Cu_2Se-In_2Se_3-Ga_2Se_3 pseudo-ternary system were identified by the XRD analysis. In our previous work [1, 2], we reported the crystal structures of $CuInSe_2$, $CuIn_3Se_5$, and $CuIn_5Se_8$ phases in the Cu-poor side of $(1-y)Cu_2Se$-yIn_2Se_3 ($0.5 \leq y \leq 1.0$) pseudo-binary system. The tie line of the $(1-y)Cu_2Se$-$y(In_{1-x}Ga_x)_2Se_3$ samples with x=0.0 and $0.5 < y \leq 1.0$ in Fig. 1 corresponds to our previous reported $(1-y)Cu_2Se$-yIn_2Se_3 system. As a result, we concluded that the crystal structure of the $(1-y)Cu_2Se$-yIn_2Se_3 sample changed from a chalcopyrite-type α-phase (y=0.5 and y=0.55) to a stannite-type β-phase ($0.60 \leq y \leq 0.75$) with increasing the content of In_2Se_3, y. The samples with $0.80 \leq y \leq 0.95$ were a mixed phase of the tetragonal β-phase and hexagonal γ-phase. Our experimental results were in good agreement with the previously reported stable phases in the Cu_2Se–In_2Se_3 pseudo-binary phase diagram [4].

In the reported phase diagram of the Cu_2Se-Ga_2Se_3 system [5], hexagonal γ-phase does not exist, but there is a wide

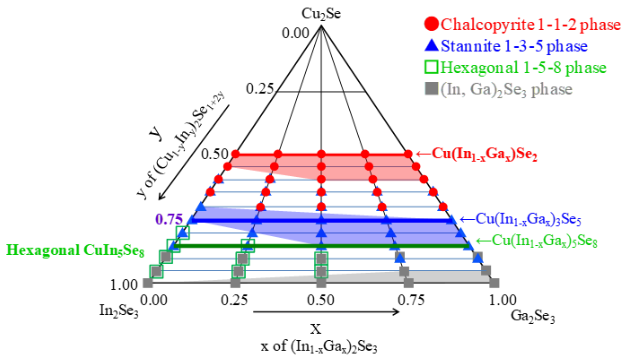

Fig. 1 Schematic crystallographic phases of $(1-y)Cu_2Se$-$y(In_{1-x}Ga_x)_2Se_3$ in Cu_2Se-In_2Se_3-Ga_2Se_3 pseudo-ternary system.

region of stannite-type β-phase (y=0.72-0.86) in the Cu-poor side of $CuGaSe_2$. In present study, the crystal structure of the $(1\text{-}y)Cu_2Se\text{-}yGa_2Se_3$ sample changed from a chalcopyrite-type ($0.50 \le y \le 0.60$) to a stannite-type ($0.75 \le y \le 0.85$) with increasing the content of Ga_2Se_3, y. The samples with $0.65 \le y \le 0.70$ were a mixture of the tetragonal chalcopyrite-type α-phase and tetragonal stannite-type β-phase. We did not observe a hexagonal γ-phase in the $(1\text{-}y)Cu_2Se\text{-}yGa_2Se_3$ system.

For the $(1\text{-}y)Cu_2Se\text{-}y(In_{1\text{-}x}Ga_x)_2Se_3$ samples, we observe that the single-phase region of the chalcopyrite-type $Cu(In_{1\text{-}x}Ga_x)Se_2$ solid solution (α-phase) increases with increasing Ga_2Se_3 content, x. Further, the single-phase region of stannite-type β-phase is also widened by replacement of In by Ga in the $(1\text{-}y)Cu_2Se\text{-}y(In_{1\text{-}x}Ga_x)_2Se_3$ samples (with increasing Ga_2Se_3 content, x). Hexagonal γ-phase is not observed in a high Ga_2Se_3 concentration ($x > 0.5$).

3.2 Band gap energies of $Cu(In_{1\text{-}x}Ga_x)Se_2$, $Cu(In_{1\text{-}x}Ga_x)_3Se_5$ and $Cu(In_{1\text{-}x}Ga_x)_5Se_8$ systems

The band-gap energies (E_gs) of the $Cu(In_{1\text{-}x}Ga_x)Se_2$ (a), $Cu(In_{1\text{-}x}Ga_x)_3Se_5$ (b) and $Cu(In_{1\text{-}x}Ga_x)_5Se_8$ (c) samples with $0.0 \le x \le 1.0$ were estimated from the $[F(R)h\nu]^2$ vs. $h\nu$ plot of the reflectance spectra. The E_g of $CuInSe_2$ (x = 0.0) in the tetragonal chalcopyrite phase is 0.99 eV. The E_g of the $Cu(In_{1\text{-}x}Ga_x)Se_2$ solid solution linearly increased from 0.99 eV of $CuInSe_2$ (x=0.0) to 1.65 eV of $CuGaSe_2$ (x=1.0) with increasing Ga content, x.

The E_g of 1.19 eV for $CuIn_3Se_5$ (x=0.0, y=0.75) with the tetragonal stannite structure is larger than that of chalcopyrite-type $CuInSe_2$ (0.99 eV) (x=0.0, y=0.50). The E_g of the $Cu(In_{1\text{-}x}Ga_x)_3Se_5$ solid solution linearly increased from 1.19 eV of $CuIn_3Se_5$ (x = 0.0) to 1.65 eV of $CuGa_3Se_5$ (x=1.0) with increasing Ga content, x. The E_g of the $Cu(In,Ga)_5Se_8$ solid solution linearly increases from 1.25 eV of $CuIn_5Se_8$ (x=0.0) to 1.91 eV of $CuGa_5Se_8$ (x=1.0) with increasing Ga content, x.

3.3 Band diagrams of $Cu(In_{1\text{-}x}Ga_x)Se_2$, $Cu(In_{1\text{-}x}Ga_x)_3Se_5$ and $Cu(In_{1\text{-}x}Ga_x)_5Se_8$ systems

Figure 2 (a) shows the band alignment of $ZnO/CdS/Cu(In_{0.5}Ga_{0.5})Se_2$ structure. For CIGSe solar cells, excellent performance can be obtained when the CBM of window layer is higher by 0-0.4eV (spike-type) than that of CIGSe. Therefore, if a high-Ga $Cu(In_{1\text{-}x}Ga_x)Se_2$ with e.g. x=0.5 is applied to an absorber layer of a CIGSe solar cell, the conduction band position of $Cu(In_{0.5}Ga_{0.5})Se_2$ is higher than that of CdS (-4.1 eV) buffer layer. The conduction band offset at the interface between CIGSe absorber and CdS buffer layers is negative. Unfavorable cliff-type conduction band offset will be formed for higher Ga content of $Cu(In_{1\text{-}x}Ga_x)Se_2$ absorber layer.

Then, we discuss the case of insertion of Cu-deficient layer of stannite-type $Cu(In_{0.5}Ga_{0.5})_3Se_5$ between $Cu(In_{0.5}Ga_{0.5})Se_2$ absorber layer and CdS buffer layer in the CIGSe solar cell. Figure 2 (b) shows the band alignment of $ZnO/CdS/Cu(In_{0.5}Ga_{0.5})_3Se_5/Cu(In_{0.5}Ga_{0.5})Se_2$ structure. As shown in Fig. 2, the band-gap energy of $Cu(In_{0.5}Ga_{0.5})_3Se_5$ increases, and the VBM becomes deeper compared with the $Cu(In_{0.5}Ga_{0.5})Se_2$. Therefore, positive valence band offset at the interface between $Cu(In_{0.5}Ga_{0.5})_3Se_5$ and $Cu(In_{0.5}Ga_{0.5})Se_2$ layers will be formed. The inserted $Cu(In_{0.5}Ga_{0.5})_3Se_5$ layer works as a hole blocking layer because the VBM of Cu deficient stannite-type $Cu(In_{0.5}Ga_{0.5})_3Se_5$ is deeper than that of chalcopyrite-type $Cu(In_{0.5}Ga_{0.5})Se_2$

Acknowledgments

This work was partially supported by NEDO under the Ministry of Economy, Trade and Industry (METI).

References

[1] T. Maeda, W. Gong, and T. Wada, Jpn. J. Appl. Phys. **55**, 04ES15 (2016).

[2] T. Maeda, W. Gong, and T. Wada, Current Opinion in Green and Sustainable Chemistry **4**, 77 (2017).

[3] T. Nishimura, Y. Hirai, Y. Kurokawa, and A. Yamada, Jpn. J. Appl. Phys. **54**, 08KC08 (2015).

[4] N. Kohara, S. Nishiawaki, T. Negami, and T. Wada, Jpn. J. Appl. Phys. 39, 6316 (2000).

[5] R. Herberholz *et al.*, Eur. Phys. J. Appl. Phys. 6, 131 (1999).

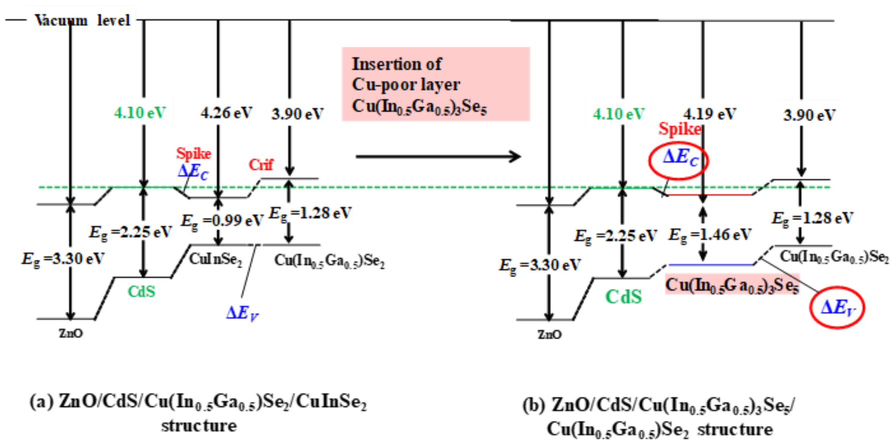

Fig. 2 Band alignment of $ZnO/CdS/Cu(In_{0.5}Ga_{0.5})Se_2$ structure with and without insertion of Cu-poor $Cu(In_{0.5}Ga_{0.5})_3Se_5$ layer.